

FUSE OBSERVATIONS OF DIFFUSE INTERSTELLAR MOLECULAR HYDROGEN

J. MICHAEL SHULL^{1,2}, JASON TUMLINSON¹, EDWARD B. JENKINS³, H. WARREN MOOS⁴, BRIAN L. RACHFORD¹, BLAIR D. SAVAGE⁵, KENNETH R. SEMBACH⁴, THEODORE P. SNOW¹, GEORGE SONNEBORN⁶, DONALD G. YORK⁷, WILLIAM P. BLAIR⁴, JAMES C. GREEN¹, SCOTT D. FRIEDMAN⁴ AND DAVID J. SAHNOW⁴

Draft version November 22, 2018

ABSTRACT

We describe a moderate-resolution FUSE mini-survey of H₂ in the Milky Way and Magellanic Clouds, using four hot stars and four AGN as background sources. FUSE spectra of nearly every stellar and extragalactic source exhibit numerous absorption lines from the H₂ Lyman and Werner bands between 912 and 1120 Å. One extragalactic sightline (PKS 2155-304) with low N(H I) shows no detectable H₂, and could be the “Lockman Hole of molecular gas”, of importance for QSO absorption-line studies. We measure H₂ column densities in low rotational states ($J = 0$ and 1) to derive rotational and/or kinetic temperatures of diffuse interstellar gas. The higher- J abundances can constrain models of the UV radiation fields and gas densities. In three optically thick clouds toward extragalactic sources, we find $n_H \approx 30 - 50 \text{ cm}^{-3}$ and cloud thicknesses $\sim 2 - 3$ pc. The rotational temperatures for H₂ at high Galactic latitude, $\langle T_{01} \rangle = 107 \pm 17$ K (seven sightlines) and 120 ± 13 K (three optically thick clouds), are higher than those in the *Copernicus* sample composed primarily of targets in the disk. We find no evidence for great differences in the abundance or state of excitation of H₂ between sight lines in the Galaxy and those in the SMC and LMC. In the future, we will probe the distribution and physical parameters of diffuse molecular gas in the disk and halo and in the lower-metallicity environs of the LMC and SMC.

Subject headings: ISM: clouds, molecules — ultraviolet: ISM — galaxies: individual (LMC, SMC)

1. INTRODUCTION

As the most abundant molecule in the Universe, molecular hydrogen (H₂) comprises the bulk of the mass of dense interstellar molecular clouds and is the main ingredient of star formation (Shull & Beckwith 1982). The first steps of star formation assemble dense interstellar clouds from diffuse gas, but the formation mechanism for giant molecular clouds from diffuse gas is still unknown. Little is known about the distribution of diffuse H₂ in the interstellar medium (ISM) of our Galaxy, and major uncertainties remain about its formation, destruction, and recycling into dense clouds and stars. H₂ also plays a central role in our understanding of interstellar chemistry.

Here, we describe early results on H₂ in the Milky Way and the Magellanic Clouds obtained with the NASA *Far Ultraviolet Spectroscopic Explorer* (FUSE) satellite. The FUSE mission and the capabilities of its spectrograph are described by Moos et al. (2000) and Sahnou et al. (2000). Over its mission lifetime, FUSE will probe hundreds of sight lines through the Galactic disk and halo. We expect a large fraction of these sight lines to exhibit absorption from the Lyman and Werner rotational-vibrational bands of H₂, some 400 absorption lines between 912 and 1120 Å, arising from rotational levels $J = 0 - 7$ in the ground vibrational state. With FUSE, our team will map the dis-

tribution of H₂ in the diffuse ISM, measure its abundance, state of excitation, and rates of formation and destruction. In § 2 we summarize our initial observations and describe our analysis methods. In § 3 we describe results from 8 targets. In § 4 we summarize our results and discuss future directions of FUSE H₂ research.

2. OBSERVATIONS AND ANALYSIS

Our FUSE observations were obtained from 1999 September to 1999 November during the commissioning phase of satellite operations. A summary of the observations appears in Table 1. The resolution of the spectrograph across the band was $R \simeq 12,000$ for all observations, based on studies of sharp interstellar lines of H₂, Ar I, and Fe II. The data were prepared for analysis by the FUSE data pipeline as described in Moos et al. (2000). Once the two-dimensional spectra were extracted to one dimension, a wavelength solution was applied and the oversampled data were smoothed by a 15-pixel running boxcar to 30 km s⁻¹ resolution.

In typical interstellar conditions, excited H₂ quickly decays to the ground vibrational state of the ground electronic state (Black & Dalgarno 1973). Observations of H₂ with the *Copernicus* satellite occasionally detected rotational lines up to $J = 7$, and we search for $J \leq 10$. How-

¹CASA, Department of Astrophysical and Planetary Sciences, University of Colorado, Boulder, CO 80309

²Also at JILA, University of Colorado and National Institute of Standards and Technology

³Department of Astrophysical Sciences, Princeton University, Princeton, NJ 08544

⁴Department of Physics and Astronomy, Johns Hopkins University, Baltimore, MD 21218

⁵Department of Astronomy, University of Wisconsin, Madison, WI 53706

⁶NASA Goddard Space Flight Center, Greenbelt, MD 20771

⁷Department of Astronomy and Astrophysics, University of Chicago, Chicago, IL 60637

ever, lines above $J = 4$ are difficult to detect in diffuse interstellar clouds, with our typical 4σ limiting equivalent width of 30–40 mÅ and the corresponding column density limit of $N(\text{H}_2) \simeq 10^{14} \text{ cm}^{-2}$. We use all available H_2 lines, except where they are blended with other interstellar absorption or airglow lines. Typically we neglect the Lyman (6-0) band, which is lost in interstellar $\text{Ly}\beta$, and the Lyman (5-0) band, which is coincident with resonance absorption lines C II $\lambda 1036.34$ and C II* $\lambda 1037.02$ and with O I $\lambda 1039.64$ airglow.

We illustrate our data in Figure 1, which displays the FUSE spectrum of ESO 141-G55, a Seyfert 1 galaxy at Galactic latitude $b = -26.71^\circ$. We detect one H_2 Galactic component with $N(\text{H}_2) = 2 \times 10^{19} \text{ cm}^{-2}$. This spectrum is typical of our FUSE data both in data quality and the abundance of H_2 lines.

We employ a complement of techniques to analyze H_2 absorption. The final products are column densities in rotational levels, $N(J)$, from which we can infer the gas density, UV radiation field, and H_2 formation and destruction rates. For high column density absorbers with damping wings in the R(0) and R(1) lines, we fit the line profiles to derive $N(0)$ and $N(1)$ and use a curve of growth to derive column densities for $J \geq 2$. For absorbers with $N(\text{H}_2) \lesssim 10^{19} \text{ cm}^{-2}$, we measure equivalent widths of all H_2 lines and produce a curve of growth to infer a doppler b -parameter and $N(J)$ – see Fig. 2. We produce initial estimates of the column densities and excitation temperatures by fitting all lines simultaneously with parameters $N(\text{H}_2)$, b , and T , assuming a Boltzmann distribution at rotational temperature T_{01} for $J = 0, 1$ and an excitation temperature T_{ex} for $J \geq 2$.

The *Copernicus* H_2 survey (Spitzer & Jenkins 1975; Savage et al. 1977) showed that the molecular fraction, $f_{\text{H}_2} = 2N(\text{H}_2)/[N(\text{H I}) + 2N(\text{H}_2)]$, is correlated with E(B-V) and with total H column density. They found that f_{H_2} undergoes a transition from low values ($\ll 0.01$) to high values (> 0.01) at $E(\text{B-V}) \approx 0.08$. Other *Copernicus* studies indicate that the populations in $J = 0, 1$ and $J \geq 2$ cannot always be described by a single excitation temperature (Spitzer, Cochran, & Hirshfeld 1974). T_{ex} is generally higher than T_{01} and reflects the fluorescent pumping of the rotational levels by incident UV radiation (Jura 1975a,b). The ratio, $N(1)/N(0)$, is usually set by collisional mixing of the ortho- and para- H_2 states (Shull & Beckwith 1982), but these rotational levels may not yet have reached equilibrium in lower density clouds.

3. RESULTS FOR INDIVIDUAL SIGHT LINES

3.1. Magellanic Cloud Targets

We report observations of one star in the LMC and three stars in the SMC. In the cases of AV 232 and HD 5980, we detect H_2 in both the Galaxy and the SMC (at $+119 \text{ km s}^{-1}$ and $+124 \text{ km s}^{-1}$; see Table 2). Our survey contains two Magellanic Cloud targets with no detected H_2 at LMC or SMC velocities. Sk -67 111 (LMC) and Sk 108 (SMC) show Galactic H_2 absorption near $v_{\text{LSR}} \approx 0$ but have no detected H_2 at the MC velocities. Our limiting equivalent width of 60 mÅ (4σ) in the Sk -67 111 spectrum sets limits $N(0) \leq 2.2 \times 10^{14} \text{ cm}^{-2}$ and $N(1) \leq 3.2 \times 10^{14} \text{ cm}^{-2}$ from the (7-0) R(0) and R(1) lines. For Sk 108, the limit of 30 mÅ yields $N(0) \leq 1.1 \times 10^{14} \text{ cm}^{-2}$ and $N(1) \leq$

$1.6 \times 10^{14} \text{ cm}^{-2}$. The absence of H_2 in these sight lines may be due to low H I columns, to intense UV radiation fields that destroy H_2 , or to reduced rates of H_2 formation on grain surfaces in warm low-metallicity gas. Abundances for such gas are given by Welty et al. (1999).

The SMC stars HD 5980 and AV 232 are separated by $75''$ on the sky. Thus, these sight lines may probe the same interstellar clouds in the Galaxy and SMC. With similar column densities and rotational temperatures, the Galactic components appear to arise in the same gas. However, the AV 232 SMC component exhibits a high rotational temperature $T_{01} = 300 \pm 60 \text{ K}$ and a higher excitation temperature $T_{\text{ex}} = 520 \pm 90 \text{ K}$, compared with $T_{01} = 98 \pm 13 \text{ K}$ and $T_{\text{ex}} = 300 \pm 60 \text{ K}$ for the HD 5980 absorber. The level populations likely arise from differing excitation rates in separate clouds, $\sim 20 \text{ pc}$ apart at the SMC.

The only detections of Magellanic Cloud H_2 absorption prior to FUSE were observations with ORFEUS (Richter et al. 1998; de Boer et al. 1998), at low signal to noise but comparable ($R \approx 10^4$) resolution. With a longer mission lifetime and higher effective area, FUSE offers significant improvement for H_2 studies. For example, with higher S/N, we do not confirm the claimed ORFEUS detections of H_2 ($J = 5, 6, 7$) at $+160 \text{ km s}^{-1}$ toward HD 5980 (Richter et al. 1998). Our observations of H_2 column densities in the $+120 \text{ km s}^{-1}$ component differ considerably, owing to a better curve of growth (Fig. 2) with $b = 10 \text{ km s}^{-1}$ compared to $b = 6 \text{ km s}^{-1}$ with ORFEUS. Based on 28 FUSE lines ($J = 0 - 3$) compared to 8 ORFEUS lines, we derive $\log N(0) = 15.10$ (compared to 16.57) and $\log N(1) = 15.30$ (compared to 15.90). Within error bars, both studies agree on $N(2)$ and $N(3)$. Our data yield $T_{01} = 98 \pm 13 \text{ K}$ for the SMC gas.

3.2. Extragalactic Targets

Our four extragalactic targets at Galactic latitude $|b| \geq 25^\circ$ probe a large volume of the Galaxy and its halo and allow us to measure the abundance and physical properties of molecular gas outside the disk for the first time. The *Copernicus* disk result, $\langle T_{01} \rangle = 77 \pm 17 \text{ K}$ (Savage et al. 1977), was drawn from 61 stars with $|b| \leq 65^\circ$. From seven FUSE sightlines, we derive $\langle T_{01} \rangle = 107 \pm 17 \text{ K}$. In the three optically thick extragalactic sightlines, $\langle T_{01} \rangle = 120 \pm 13 \text{ K}$. These results may indicate a higher level of rotational excitation in the upper disk and low halo, which could arise from more intense UV pumping or photoelectric heating from grains in the infrared cirrus. However, these interpretations are still speculative, since the the $J = 0, 1$ levels may not be in equilibrium with the kinetic temperature as a result of UV radiative pumping.

In general, the H_2 rotational populations can be modeled (Jura 1975a,b) to provide physical diagnostics of H_2 -bearing clouds, such as n_{H} , T_{01} , thermal pressure, and UV radiation field. We also derive internally consistent values of $N(\text{H}_2)$ and T_{ex} for these clouds, which could indicate the presence of warm H_2 -bearing gas in the lower Galactic halo. For the three AGN sightlines with detectable H_2 , we find $n_{\text{H}} = 50, 50,$ and 36 cm^{-3} for Mrk 876, ESO 141-G55, and PG 0804+761 respectively, which yields cloud thicknesses of 1.9, 2.4, and 3.3 pc. The line of sight to ESO 141-G55 intersects a region of enhanced *IRAS* 100 μm emission (Sembach, Savage, & Hurwitz 1999). The other extragalactic sightlines lie behind high-velocity cloud Complex

C (Mrk 876) and weak infrared cirrus (PG 0804+761). Our H₂ results suggest that these clouds are also compressed.

4. SUMMARY AND FUTURE DIRECTIONS

The major results of these early FUSE observations are: (1) the ubiquity of H₂ in nearly all sightlines; (2) the generally warmer rotational temperatures, T_{01} toward high-latitude gas; and (3) the presence of one low-H₂ extragalactic sightline (PKS 2155-304). We have not detected H₂ in the high velocity clouds (HVCs) toward Mrk 876 or PKS 2155-304, although we intend to continue our HVC searches toward other targets. The HD molecule was not detected in any diffuse cloud, but results from a complementary program (Snow et al. 2000; Ferlet et al. 2000) detect H₂ and HD toward the reddened star HD 73882. Detections of H₂ in other FUSE sight lines are analyzed by Friedman et al. (2000), Mallouris et al. (2000), and Oegerle et al. (2000).

The lack of detectable H₂ toward PKS 2155-304 is quite interesting, in contrast to the general presence of H₂ at high Galactic latitudes. Extragalactic sight lines with low H₂ are valuable for studies of QSO absorption lines (Shull et al. 2000; Sembach et al. 2000), since H₂ line blanketing can add confusion to line identifications (Fig. 1). The observed low N(H₂) may reflect the intrinsic patchiness of the ISM, but can also be influenced by H₂ formation/destruction in regions of high UV radiation fields and low hydrogen column density. PKS 2155-304 has the lowest column density, $\log N(\text{H I}) \approx 20.15$, of any of our targets. The Sk 108 sight line shows no H₂ at SMC veloc-

ities, and the Sk -67 111 sight line shows no H₂ at LMC velocities. Although H₂ formation may not reach equilibrium with UV destruction in these diffuse clouds, the H₂ formation rate could depend on the metallicity through the content of dust grains, whose surfaces catalyze H₂ formation. In the Galactic halo, some clouds may be exposed to strong UV dissociating radiation from OB associations in the disk. With more sight lines, we should be able to correlate regions lacking H₂ with regions of low N(H I) and low metallicity (LMC, SMC). Close sight lines such as those to HD 5980 and AV 232 present an opportunity to probe the size of diffuse H₂-bearing interstellar clouds.

The primary product of future FUSE diffuse H₂ studies will be a map of the distribution of diffuse clouds in the disk and halo of the Milky Way, using a large sample of sight lines toward Galactic and extragalactic targets. Multiple sight lines to the Magellanic Clouds will permit the study of CO/H₂ and possibly HD/H₂ in lower-metallicity environs, including high-velocity clouds in the Galactic halo and Magellanic Stream (Gibson et al. 2000). Observations of multiply-intersected absorbers and H₂ associated with infrared cirrus and high velocity clouds can constrain the size of these diffuse interstellar clouds.

This work is based on data obtained for the Guaranteed Time Team by the NASA-CNES-CSA FUSE mission operated by the Johns Hopkins University. Financial support to U.S. participants has been provided by NASA contract NAS5-32985. J.M.S. also acknowledges the support of NASA astrophysical theory grant NAG5-4063.

REFERENCES

- Black, J. H., & Dalgarno, A. 1973, *ApJ*, 184, L101
 de Boer, K. S., et al. 1998, *A&A*, 338, L5
 Dickey, J., & Lockman, F. J. 1990, *ARA&A*, 28, 215
 Ferlet, R., et al. 2000, *ApJ*, this issue
 Friedman, S. D., et al. 2000, *ApJ*, this issue
 Gibson, B. K., Giroux, M. L., Penton, S. V., Putman, M., Stocke, J. T., & Shull, J. M. 2000, *AJ*, submitted
 Jura, M. 1975a, *ApJ*, 197, 575
 Jura, M. 1975b, *ApJ*, 197, 581
 Mallouris, C., et al. 2000, *ApJ*, in preparation
 Moos, H. W., et al. 2000, *ApJ*, this issue
 Oegerle, W. R., et al. 2000, *ApJ*, this issue
 Richter, P., et al. 1998, *A&A*, 338, L9
 Sahnou, D. et al. 2000, *ApJ*, this issue
 Savage, B. D., & deBoer, K. S. 1981, *ApJ*, 243, 460
 Savage, B. D., Bohlin, R. C., Drake, J. F., & Budich, W. 1977, *ApJ*, 216, 291
 Sembach, K. R., et al. 2000, *ApJ*, in preparation
 Sembach, K. R., Savage, B. D., & Hurwitz, M. 1999, *ApJ*, 524, 98
 Shull, J. M., Giroux, M. L., et al. 2000, *ApJ*, this issue
 Shull, J. M., & Beckwith, S. V. W. 1982, *ARA&A*, 20, 163
 Snow, T. P., et al. 2000, *ApJ*, this issue
 Spitzer, L., Jr., Cochran, W. D., & Hirshfeld, A. 1974, *ApJS*, 28, 373
 Spitzer, L., Jr., & Jenkins, E. B. 1975, *ARA&A*, 13, 133
 Welty, D., et al. 1999, *ApJ*, 512, 636

TABLE 1
FUSE H₂ MINI-SURVEY TARGET LIST

Target	Channels ¹	t_{exp} (N) ² (ksec)	S/N ³
Mrk 876	L1 L2 S1	45.9 (10)	15
ESO 141-G55	L1 L2 S2	35.8 (20)	15
PG 0804+761	L1 L2 S1	39.6 (12)	15
Sk -67 111 (LMC)	L1	13.8 (7)	15
AV 232 (SMC)	L1	10.3 (5)	12
HD 5980 (SMC)	L1	3.2 (8)	15
Sk 108 (SMC)	L1	13.3 (8)	30
PKS 2155-304	L1 L2 S2	37.1 (22)	20

¹Detectors LiF (L1 and L2 channels) and SiC (S1 and S2 channels) have wavelength ranges described by Moos et al. (2000).

²Exposure time and number (N) of sub-exposures.

³Signal-to-noise ratio per smoothed (30 km s⁻¹) bin between 1040–1050 Å.

TABLE 2
FUSE H₂ MINI-SURVEY RESULTS ¹

Name (Type)	l (°)	b (°)	v_{LSR} (km s ⁻¹)	N(H ₂) (cm ⁻²)	N(H I) (cm ⁻²)	f_{H2}	T_{01} (K)	T_{ex} (K)	b_{dopp} (km s ⁻¹)
<i>Magellanic Cloud Sight Lines</i>									
Sk -67 111 (LMC, O7)	277.75	-32.97	0	2.3×10^{15}	6.2×10^{20}	7.4×10^{-6}	122	300	8
			+270	$<5.5 \times 10^{14}$
AV 232 (SMC, O9)	302.06	-44.94	0	1.6×10^{16}	3.6×10^{20}	8.9×10^{-5}	86	195	5
			+119	2.0×10^{15}	300	520	7
HD 5980 (SMC, WR)	302.07	-44.95	0	9.8×10^{15}	3.6×10^{20}	5.4×10^{-5}	98	195	5
			+124	4.2×10^{15}	98	300	10
Sk 108 (SMC, WR)	301.63	-44.99	0	1.1×10^{16}	3.4×10^{20}	6.5×10^{-5}	85	180	7
			+120	$<2.7 \times 10^{14}$
<i>Extragalactic Sight Lines</i>									
Mrk 876 (Seyf1)	98.27	40.38	0	2.3×10^{18}	2.7×10^{20}	1.7×10^{-2}	135	200	5
ESO 141-G55 (Seyf1)	338.18	-26.71	0	1.9×10^{19}	3.5×10^{20}	9.3×10^{-3}	113	540	10
PG 0804+761 (QSO)	138.28	31.03	0	6.1×10^{18}	3.5×10^{20}	3.4×10^{-2}	113	180	8
PKS 2155-304 (BL Lac)	17.73	-52.27	...	$<4.6 \times 10^{14}$	1.4×10^{20}	$<6.6 \times 10^{-6}$

¹Columns: Target name (type); Galactic coordinates (e at l , b); H₂ absorber velocity in LSR (Galactic H₂ is assumed to lie at 0 km s⁻¹ in LSR); column densities of H₂ (typically ± 0.2 dex from FUSE) and H I (21 cm emission, Dickey & Lockman 1990; Lockman, Murphy, & Sembach, in preparation; Savage & deBoer 1981; Sembach, Savage, & Hurwitz 1999); molecular fraction, $f_{\text{H2}} = 2N(\text{H}_2)/[N(\text{H I}) + 2N(\text{H}_2)]$; rotational temperature T_{01} (typically ± 15 K) from $J = 0$ and 1; excitation temperature T_{ex} (typically ± 75 K) from $J \geq 2$; and doppler parameter (typically ± 2 km s⁻¹) from H₂ curve of growth.

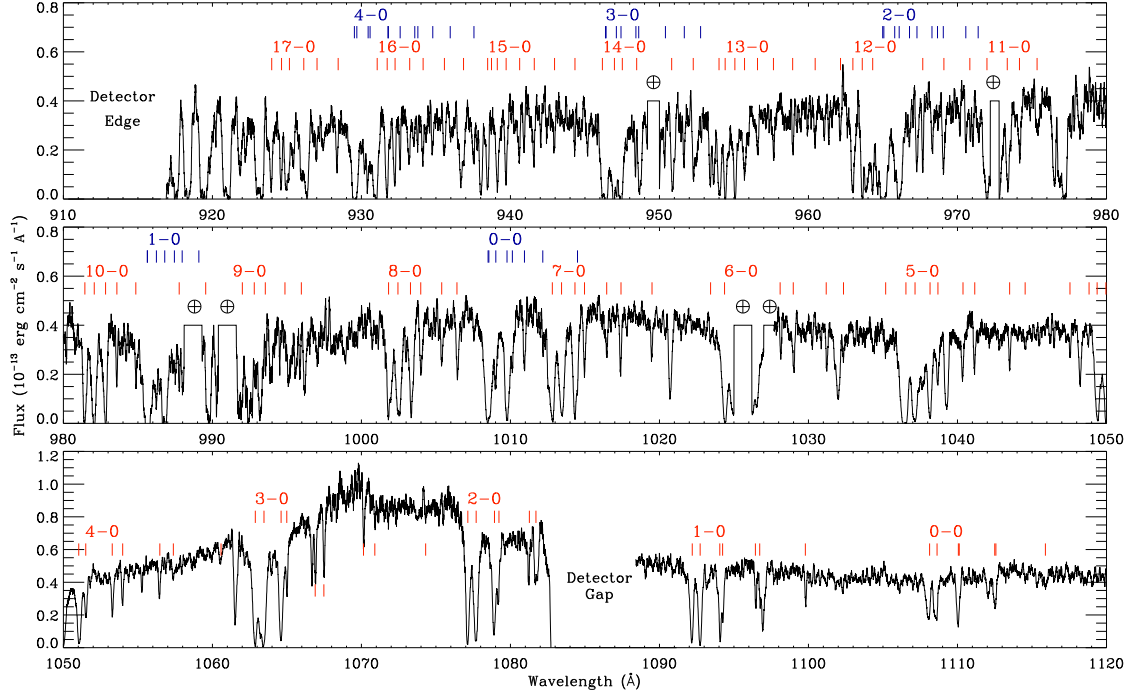


FIG. 1.— FUSE spectrum of ESO 141-G55. Bright airglow lines have been truncated. This spectrum has a resolution of $R \simeq 12,000$ and $S/N \approx 15$ per smoothed (30 km s^{-1}) bin (1040–1050 Å) and $S/N \approx 25$ at 1070 Å. Lower (red) and upper (blue) ticks mark the detected Lyman and Werner lines of H_2 , respectively. The interstellar and intergalactic lines are analyzed further by Sembach et al. (2000) and Shull et al. (2000).

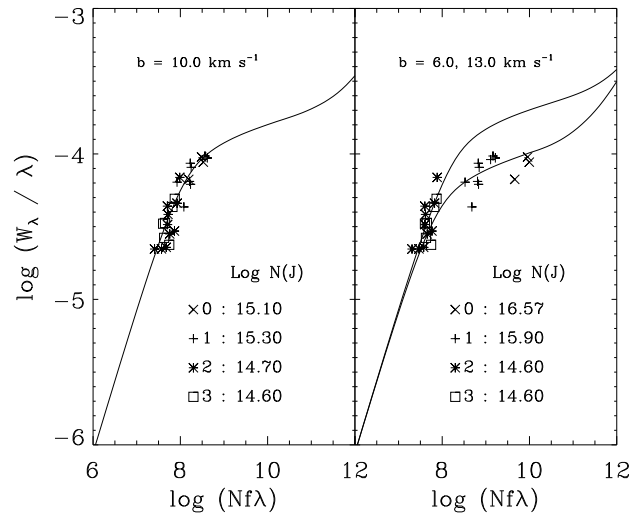


FIG. 2.— (Left) Composite curve of growth for 28 H_2 lines ($J = 0, 1, 2, 3$) in the SMC ($+120 \text{ km s}^{-1}$) component toward HD 5980 with best-fit doppler parameter, $b = 10 \text{ km s}^{-1}$, and column densities, $N(J)$. (Right) Same 28 FUSE lines but with the higher ORFEUS column densities (Richter et al. 1998, who used $b = 6 \text{ km s}^{-1}$).